

Air Shower Simulations in a Hybrid Approach using Cascade Equations

Hans-Joachim Drescher and Glennys R. Farrar
Center for Cosmology and Particle Physics
Department of Physics, New York University
4 Washington Place, New York, NY 10003

A new hybrid approach to air shower simulations is described. At highest energies, each particle is followed individually using the traditional Monte Carlo method; this initializes a system of cascade equations which are applicable for energies such that the shower is one-dimensional. The cascade equations are solved numerically down to energies at which lateral spreading becomes significant, then their output serves as a source function for a 3-dimensional Monte Carlo simulation of the final stage of the shower. This simulation procedure reproduces the natural fluctuations in the initial stages of the shower, gives accurate lateral distribution functions, and provides detailed information about all low energy particles on an event-by-event basis. It is quite efficient in computation time.

I. INTRODUCTION

The field of highest energy cosmic rays is an exciting subject with many open questions: What is the nature of the primary cosmic ray? What are the highest energies? What are possible sources/acceleration mechanisms? Is there clustering of events? Is there a GZK cutoff due to the microwave background? Ongoing (HIRES, AGASA) and future (Auger, OWL, EUSO) cosmic ray experiments aim to shed light on these mysteries.

At these high energies, direct measurement of the primary cosmic ray is impossible due to the low flux, which is only of order one event per square-kilometer per century at the highest observed energies. But cosmic rays initiate showers in the atmosphere, a cascade of secondary particles from collisions with air molecules, which themselves collide and so on. Experiments measure these air showers and reconstruct from their properties information about the primary ray at the beginning of the reaction.

Air shower models are of crucial importance for the reconstruction of the energy and primary type. The straightforward approach is to model each possible interaction of hadrons, leptons and photons with air molecules, and trace all secondary particles. At high energies this leads quickly to unpractical computation times, since the time grows with the number of particles in the shower and therefore increases rapidly with the primary energy. A shower of even $10^{19}eV$ has more than 10^{10} particles at its maximum and would take months to compute. The thinning algorithm proposed by Hillas [1] tries to solve this problem: below a fraction f_{thin} of the primary energy only a small sample of the particles is actually followed in detail, attributing them a higher weight. This procedure introduces artificial fluctuations and one must compromise between these and computation time.

People have tried to overcome these difficulties by defining systems of (mostly one-dimensional) transport equations which describe air showers [2, 3]. The numerical solutions of these equations can then be combined with a Monte-Carlo in order to account for natural fluctu-

ations due to the first interactions and for lateral spread of low-energy particles [4, 5]. This is the principle of the hybrid method. Another realization of the hybrid approach is to use shower libraries in which presimulated longitudinal profiles are combined to compute the one-dimensional properties of air showers [6, 7].

In a recent paper [8], a new approach to an old idea was introduced: the method of cascade equations, which allows one to compute longitudinal characteristics of air showers numerically in a very short time.

In this paper we introduce the further development of this approach. Traditional Monte-Carlo methods are combined with cascade equations in a hybrid approach. This allows to construct an efficient model which accounts not only for natural fluctuations due to the first interactions but also for the correct 3-dimensional spreading of low-energy secondary particles. In reasonable computing time it is possible to calculate longitudinal profiles and lateral distribution functions with detailed knowledge about particle momenta and arrival-times, which are reliable on an event-by-event basis.

II. HYBRID APPROACH TO AIR SHOWER MODELING

The solution of one-dimensional cascade equations cannot account for natural fluctuations or the lateral spread of particles. The fluctuations can be, as already suggested, solved by doing the first interactions up to a certain fraction f of primary energy E_0 , in a classical Monte-Carlo approach, where each collision is treated individually by the chosen hadronic model. All secondary particles below the critical energy fE_0 are not followed further on, but taken to be initial conditions for the hadronic cascade equations.

The one-dimensional cascade equations are only valid for large enough energies that the emission angles of secondaries can be neglected, and the whole problem can be treated longitudinally. Therefore the lateral spreading of particles cannot be treated in this approach and we return to the Monte Carlo method for the low energy regime. At E_{min} , the output of the cascade equations

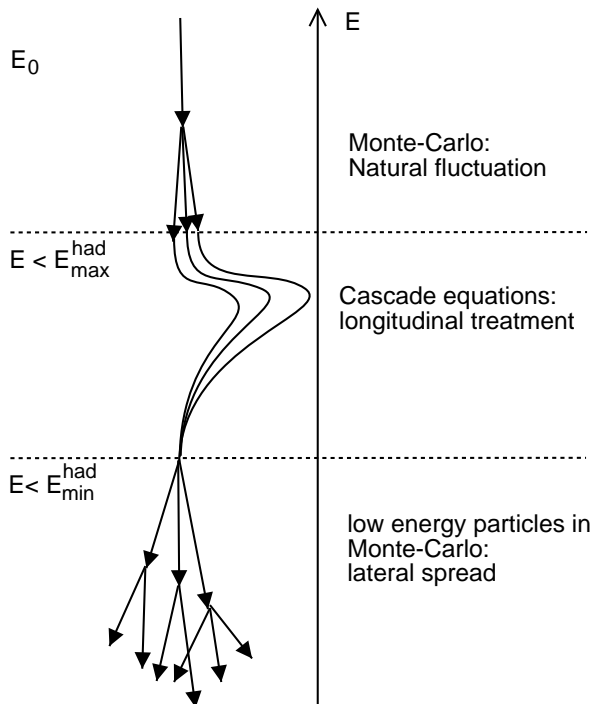


FIG. 1: Schematic illustration of the hybrid approach using cascade equations.

– the number of particles at certain depths and energies – is used as a source function for the Monte Carlo approach, by creating single particles according to the source function and following them individually. This method is able to reproduce the lateral spread of secondary particles even though it is neglected for collisions with $E > E_{\min}^{\text{had}}$.

Fig. 1 illustrates schematically the hybrid approach.

Throughout this paper, which concentrates on establishing the validity of the technique, we use QGSJET [9] as high energy hadronic model. Low energy hadrons are treated by GHEISHA [10]. The electromagnetic part is calculated by the EGS4-code system [11]. The bremsstrahlung and e^{\pm} pair-production by muons is done using the GEANT3.21 code [12]. At this stage we neglect the LPM effect, muon-pair production and photo-nuclear reactions. These effects are essentially negligible for hadron primaries [7, 13, 14]. The program embodying this method which was used for the calculations presented in this paper, SENECA, is available for public use at <http://cosmo.nyu.edu/~hjd1/SENECA/>.

III. HADRONIC CASCADE EQUATIONS

In the domain of applicability of the cascade equations, the shower is one-dimensional and relativistic. Therefore it is completely specified by h_n , where $h_n(E, X)dE$ is the number of particles of a given species n with energy in the range $[E, E + dE]$, at an atmospheric slant depth

X (with $X = \int \rho_{\text{air}}(x)dx$). The reaction probability of a particle in the atmosphere is given by its interaction length and decay length, so

$$\frac{dh_n(E, X)}{dX} = -\frac{h_n(E, X)}{\lambda_n(E)} - \frac{1}{c\tau_n\gamma\rho_{\text{Air}}}h_n(E, X), \quad (1)$$

where $\lambda_n(E)$ is the mean free path, τ_n the lifetime of the particle and γ its Lorentz-factor. By writing $\rho_{\text{Air}} = \rho_0 \exp(-h/h_0) = X/h_0$, one can rewrite these equations as

$$\frac{dh_n(E, X)}{dX} = -\frac{h_n(E, X)}{\lambda_n(E)} - \frac{B_n}{EX}h_n(E, X) \quad (2)$$

where B_n is the decay constant of hadron n defined by

$$B_n = mc^2h_0/c\tau_n. \quad (3)$$

Accounting for particles produced at higher energies gives rise to the following system of hadronic cascade equations[8]

$$\begin{aligned} \frac{\partial h_n(E, X)}{\partial X} = & -h_n(E, X) \left[\frac{1}{\lambda_n(E)} + \frac{B_n}{EX} \right] \\ & + \sum_m \int_E^{E_{\max}^{\text{had}}} h_m(E', X) \left[\frac{W_{mn}(E', E)}{\lambda_m(E')} \right. \\ & \left. + \frac{B_m D_{mn}(E', E)}{E'X} \right] dE'. \end{aligned} \quad (4)$$

Most important are the functions $W_{mn}(E', E)$, which are the energy-spectra $\frac{dN}{dE}$ of secondary particles of type n in a collision of hadron m with air-molecules. $D_{mn}(E', E)$ are the corresponding decay-functions. Equation (4) is a typical transport equation with a source term. The first term with the minus-sign accounts for particles disappearing by collisions or decays, whereas the source term accounts for production of secondary particles by collisions or decays of particles at higher energies. The technique for the solution is explained in detail in reference [8] and we discuss in the following only two major changes.

First, the discretized functions

$$W_{mn}^i(E^j) = \int_{E_i/\sqrt{c}}^{E_i \cdot \sqrt{c}} \frac{E}{E_i} W_{mn}(E^j, E') dE' \quad (5)$$

are not calculated by fitting the functions W_{mn} to the energy-spectrum given by the hadronic Monte Carlo model, but by direct counting of the number of particles falling in the energy-bin defined by the limits of the integral in equation 5. This gives the desired precision as long as the number of simulated events is high, and avoids introducing systematic errors due to the fitting procedure. The binning of the discrete energies is

$$E_i = 1 \text{ GeV} \times 10^{\frac{i-1}{n^{\text{had}}}},$$

meaning n_d^{had} logarithmic bins per decade. A typical value is 10, but as we will see below, a higher value can be preferable for some applications.

Second, the equations are modified to account for an arbitrary atmospheric density, since a real atmospheric profile is somewhat more complicated than the simple exponential form. Since the cascade equations are solved in layers $X_i, X_{i+1} = X_i + \Delta X, \dots$ with, typically, $\Delta X = 2.5 \text{ g/cm}^2$, one can approximate the density in each layer as

$$\rho_{\text{Air}} = a_i + b_i X \text{ for } X_i < X \leq X_{i+1}. \quad (6)$$

The parameters a_i and b_i can easily be calculated from any function of the density. Dropping the indices, function (2) becomes

$$\frac{dh_n(E, X)}{dX} = -\frac{h_n(E, X)}{\lambda_n(E)} - \frac{B_n/h_0}{E(a + bX)} h_n(E, X) \quad (7)$$

which has the solution

$$h_n(E, X) = C \exp(-X/\lambda) (a + bX)^{-\frac{B_n}{h_0 E b}}, \quad (8)$$

where $a = a_i$ and $b = b_i$ when X is in the range $X_i < X \leq X_{i+1}$. Defining the corresponding cascade equations is then straightforward. This generalization allows one not only to implement different atmospheres but also to solve for horizontal showers due to neutrino interactions in the atmosphere.

The initial condition for the cascade equation for a particle of type m and energy E_m at depth X_m is given by:

$$h_n(E, X = X_m) = \delta_{nm} \delta(E - E_m). \quad (9)$$

The initial condition for the cascade equation is thus in general a superposition of many functions like (9), which accounts for the natural fluctuations.

To recapitulate, down to a certain fraction $f^{\text{had}} = E_{\text{max}}^{\text{had}}/E_0$ of the primary energy, all particles are followed with Monte Carlo method, meaning that each collision is simulated explicitly by the underlying event generator. Particles falling below $E_{\text{max}}^{\text{had}}$ are filled into the initial condition $h_n(E, X)$. After all particles above $E_{\text{max}}^{\text{had}}$ are processed, one can then proceed by solving the cascade equations.

IV. ELECTROMAGNETIC CASCADE MODELING

The electromagnetic part of the air-shower in reference [8] was calculated with the analytic NKG formula. This is advantageous for the speed of the computation but it has some disadvantages: one has no detailed knowledge of particle spectra and it introduces inaccuracies since the NKG formula is only an approximation. The Monte

Carlo approach can be used – e.g., the EGS4 [11] package provides a detailed Monte Carlo model for electromagnetic showers in any medium – but it is very time consuming for higher energies. We therefore apply the same approach as for hadronic cascades, by defining a system of electromagnetic cascade equations, analogous to (4). Due to the fact that e^\pm and photons do not decay, the equations simplify greatly by setting the decay constants B to zero. This basically means that the showering is independent of altitude if one considers path lengths in units of g/cm^2 . This fact allows a further simplification: First one defines energy-bins by

$$E_i = 1 \text{ GeV} \times 10^{\frac{i-1}{n_{\text{d,em}}}}$$

the limits of each bin being

$$E_i 10^{\frac{-0.5}{n_{\text{d,em}}}} < E \leq E_i 10^{\frac{+0.5}{n_{\text{d,em}}}}.$$

One defines V_{ij}^{mn} as the number of particles of type n ($1=\text{photon}, 2=\text{electron/positron}$) in energy bin E_j generated in a electromagnetic shower induced by particle m of energy E_i , traversing a layer of air with thickness ΔX of the order of some g/cm^2 . This means $V_{ij}^{mn} = V_{ij}^{mn}(\Delta X)$ is a function of layer thickness ΔX . In our case we choose $\Delta X = 2.5 \text{ g/cm}^2$.

Let $g_i^n(X)$ be the number of particles of type n and energy E_i at a given depth X . Then,

$$g_i^n(X + \Delta X) = \sum_{m, j > i} g_j^m(X) V_{ji}^{mn}(\Delta X).$$

The function $V_{ji}^{mn}(\Delta X)$ can be calculated in reasonable time by the showering model EGS4 since ΔX is quite small. Once calculated, $V_{ji}^{mn}(\Delta X)$ is stored as a table, and can be used to calculate efficiently any electromagnetic shower.

V. LOW ENERGY SOURCE-FUNCTIONS

We wish to follow particles down to an energy E_{cut} , below which they produce a negligible signal in the detector. Air showers have a lateral expansion of secondary particles, so the approach of 1-D cascade equations is certainly wrong for calculating particles down to lowest energies. Therefore, we employ the CE only to a certain minimum energy, $E_{\text{min}}^{\text{had}}$ and $E_{\text{min}}^{\text{em}}$ for hadronic and electromagnetic showers respectively. These are parameters which are determined empirically as described in the next section. The cases of electromagnetic and hadronic showers are analogous, so we describe the hadronic case for definiteness here.

Particles with energies $E < E_{\text{min}}^{\text{had}}$, produced in collisions with $E \geq E_{\text{min}}^{\text{had}}$ contribute to the source function $h_n^{\text{source}}(E, X)$ which is the number of produced particles at depth X and energy E . It obeys the equation

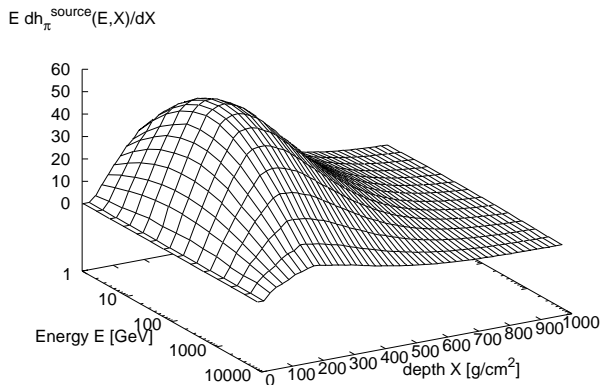


FIG. 2: An example for a source function of π^\pm . $E \frac{\partial h_n^{\text{source}}(E,X)}{\partial X}$ is plotted which means the number of produced particles per logarithmic energy bin $d \ln(E)$ and depth dX .

$$\frac{\partial h_n^{\text{source}}(E,X)}{\partial X} = \sum_m \int_{E_{\text{min}}^{\text{had}}}^{E_{\text{max}}^{\text{had}}} h_m(E',X) \left[\frac{W_{mn}(E',E)}{\lambda_m(E')} + \frac{B_m D_{mn}(E',E)}{E'X} \right] dE'. \quad (10)$$

The first term from equation (4) is missing because the propagation of these will be described by a Monte Carlo method.

An example of a typical source function of pions for a vertical 10^{19}eV proton induced shower is given in Fig. 2, choosing $E_{\text{min}}^{\text{had}} = 10^4 \text{ GeV}$. The source function is used to generate particles, which are then traced in the Monte-Carlo part of the air shower simulation code. With unlimited computational speed, the number $N_n = \int_{E_{\text{cut}}^{\text{had}}}^{E_{\text{min}}^{\text{had}}} \int \frac{h_n^{\text{source}}(E,X)}{\partial X} dE dX$ of particles would be produced for each species n , however at high energies this is time consuming. Instead, only a certain fraction of the total number of particles is sampled, attributing to each particle a suitable weight larger than 1. A practical way to define the sampling procedure is to specify the total amount of hadronic (or em) energy which is carried by the particles followed in the low energy MC. Because computation time is roughly proportional to energy, this procedure allows one to achieve equally good statistics independent of the energy E_0 of the primary cosmic ray. To be precise, the procedure is the following. The total energy of hadrons in the low energy regime produced by reactions with energy greater than $E_{\text{min}}^{\text{had}}$ is $E_{\text{low,tot}}^{\text{had}} = \sum_n \int_{E_{\text{cut}}^{\text{had}}}^{E_{\text{min}}^{\text{had}}} \int E \frac{h_n^{\text{source}}(E,X)}{\partial X} dE dX$, with the index n summing over the particle types. If low energy particles distributed according to the source function would be generated until their energy totalled $E_{\text{low,tot}}^{\text{had}}$, the weight would be 1. Instead we produce par-

method	thinning level f_{th}	CPU-time[min]
MC	10^{-5}	71
	10^{-6}	383
	10^{-7}	2148
CE		19

TABLE I: CPU time comparison for the showers shown in Fig. 3. The showers have been calculated on a 1.266Ghz processor.

ticles until their total energy is $E_{\text{low}}^{\text{had}} < E_{\text{low,tot}}^{\text{had}}$, so the weight attributed to each particle is $w = \frac{E_{\text{low,tot}}^{\text{had}}}{E_{\text{low}}^{\text{had}}} > 1$. With this method, a simple adjustment of $E_{\text{low}}^{\text{had}}$ controls the final weight of all particles, since the shower of each generated particle is followed in full detail with no further thinning. Thus this method also overcomes a weakness of the normal thinning method, where the weight itself can fluctuate a lot.

It can happen that particles with $E < E_{\text{min}}^{\text{had}}$ are produced in the high energy MC stage, in reactions with particles of an energy $E > E_{\text{max}}^{\text{had}}$. Following all of these with weight 1 down to $E_{\text{cut}}^{\text{had}}$ is time consuming and unnecessary for particles with angle less than about $\approx 5^\circ$ with respect to the shower axis. These are stored in the low energy source function and re-appear in the computation at the stage when low energy particles are created from the source function as discussed above. Low energy particles with larger angles are treated directly in the Monte Carlo part.

Neutral pions have a very short decay length and are therefore treated separately. In the system of cascade equations (4), they appear only as secondary particles and formula (10) is evaluated for $E < E_{\text{max}}^{\text{had}}$. The resulting π^0 s can then be fed either into the electromagnetic cascade equations for $E > E_{\text{min}}^{\text{em}}$ or into the Monte Carlo part of the code for $E \leq E_{\text{min}}^{\text{em}}$. This approach is valid for $E_{\text{max}}^{\text{had}} < B_{\pi^0} = 3 \times 10^{19} \text{ eV}$.

The generalization of the source function method to the electromagnetic case is straightforward.

VI. TESTS AND APPLICATIONS

In the ideal case all the methods described here are just of technical nature, which means that the final result of physical observables of air showers should not depend on whether they are calculated with the traditional Monte Carlo (MC) method or with the hybrid method proposed here, using cascade equations (CE). Therefore a first step is to check the new technique by comparing the results of the two approaches and the influence of the parameters $E_{\text{min}}^{\text{had}}$ and $E_{\text{min}}^{\text{em}}$ on longitudinal and lateral profiles. In a second step we show some comparisons to the CORSIKA model, which can be configured to use the same external models - QGSJET, GHEISHA and EGS4.

Before doing so we show a comparison of the com-

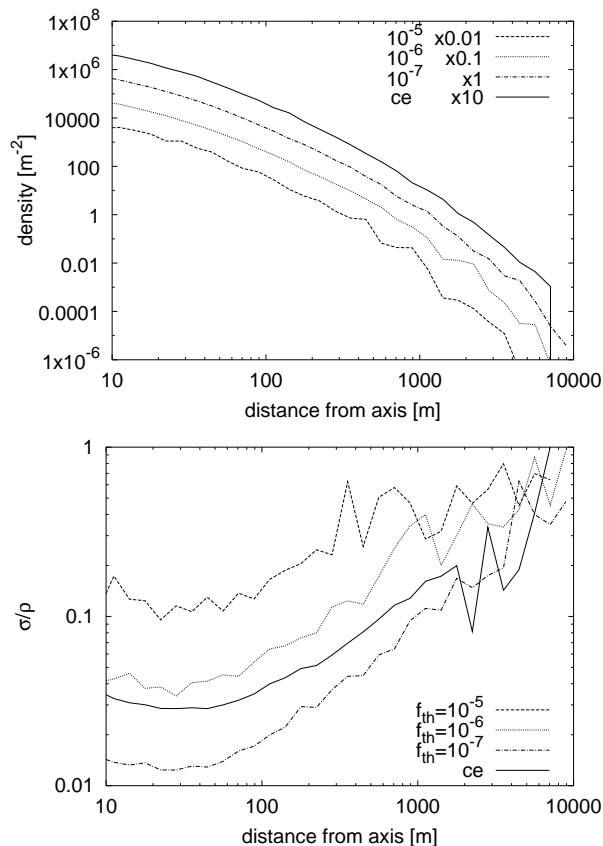


FIG. 3: The lateral distribution function of showers calculated with cascade equations and Monte Carlo using thinning. The bottom figure shows the relative fluctuations σ/ρ .

putation time necessary to simulate $10^{19}eV$ proton induced vertical showers in table I. The results of CE using $E_{low}^{had} = 10^6 GeV$ and $E_{low}^{em} = 10^5 GeV$ are compared with a pure traditional Monte-Carlo method using various thinning levels f_{thin} ($f_{thin}E_0$ is the energy below which only one secondary i in each reaction is followed with probability $p_i = E_i/\sum_i E_i$ having a weight $w_i = 1/p_i$).

The corresponding lateral distribution functions and the relative fluctuations can be seen in Fig. 3. The relative fluctuations in each lateral bin are defined by

$$\frac{\sigma}{\rho} = \frac{\sqrt{\sum w_i^2}}{\sum w_i}, \quad (11)$$

where w_i is the weight of particle i . One sees in Fig. 3 that the quality of the LDF computed with CE is somewhere between the thinning levels 10^{-6} and 10^{-7} (approaching the latter for large distances), whereas the computation time is at least 20 times lower as seen in table I. As the energy of the primary cosmic ray is increased, the CPU time of the CE stays approximately constant if one keeps the same values for E_{low}^{had} and E_{low}^{em} . This is because most of the time is used for the low energy Monte Carlo part. In the pure MC method, higher values

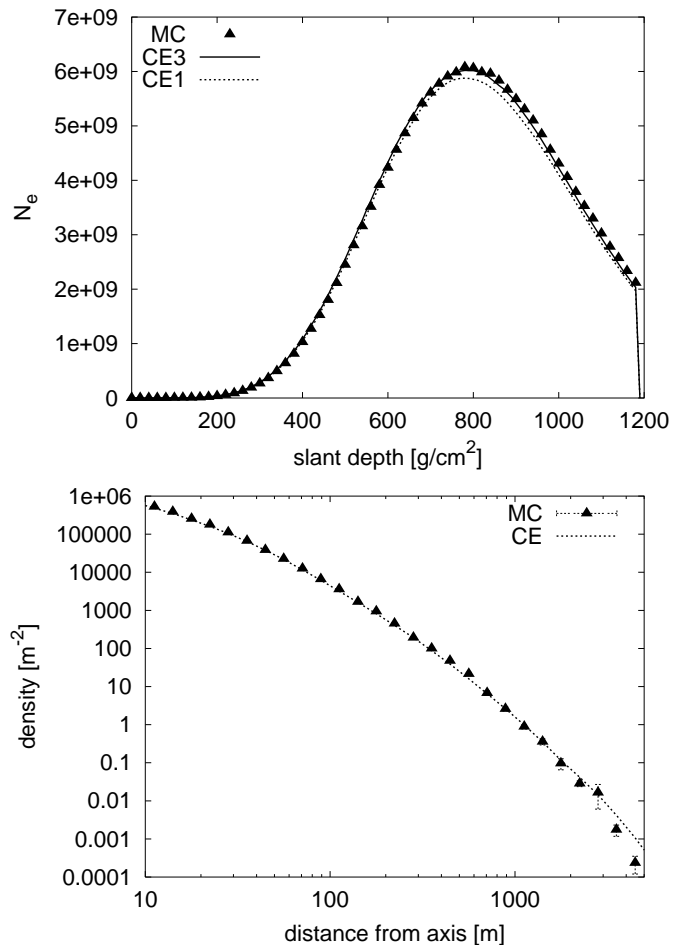


FIG. 4: Comparison of longitudinal and lateral profiles using the MC and CE approaches (upper and lower figures, respectively). CE1 denotes cascade equations with 10 bins per decade, CE3 with 30. There is no noticeable difference in the LDF for different binnings; these are therefore not shown.

of the thinning parameter f_{thin} can often be used while maintaining the statistical quality, so the improvement factor using the CE grows only slowly at higher energies. For instance, at $3 \times 10^{20}eV$, $f_{thin} = 10^{-6}$ gives results comparable to the CE approach using the same values for E_{low}^{had} and E_{low}^{em} with a time difference of a factor of about 40.

A. Checks on an average shower basis

If one applies the cascade equations starting from the primary energy, an average shower is calculated. In this case the initial condition consists just of the primary cosmic ray. We can compare such a result to the average of many showers computed by the MC-method. Fig. 4 shows such a comparison for $10^{19}eV$ proton induced vertical showers. The lateral and longitudinal profiles agree nicely within a small error. The shower maxima X_{max}

agree within less than 1%. As for the shower size N_{max} (number of particles at shower maximum), we achieve 3% accuracy if we use 10 bins per decade in the numerical solution, but this can be improved to 1% by using 30 bins instead.

The other relevant parameters of the CE are $E_{min}^{had} = 10^4 GeV$, $E_{min}^{em} = 10 GeV$. The performance of the CE depends on these parameters as well as on the binning chosen for the numerical solution. A fine binning takes a long time to compute, whereas a more rough binning might introduce a significant error. Similarly, minimizing computation time argues for a low energy threshold E_{min} for both cascades, but not too low in order to obtain accurate lateral distribution functions. In the following we are going to analyze the influence of these parameters on the performance of the CE.

1. E_{min}^{em}

The lower threshold E_{min}^{em} should be chosen in the region where the electromagnetic shower cannot be treated anymore as one-dimensional, and the lateral spread of electrons, positrons and photons becomes important. Fig. 5 shows the longitudinal and lateral profiles for different values of E_{min}^{em} . As of a threshold of 10 GeV, the profiles do not change significantly anymore. A very similar approach was used in reference [5]. There, a more complicated set of cascade equations was solved which involved also angular deviations from the shower-axis, and secondary particles below 10 GeV were followed in a MC method. Here we see that it is sufficient to treat the problem above 10 GeV in a purely longitudinal way.

2. E_{min}^{had}

Analogously to the lower threshold in electromagnetic CE, the proper choice of the lower threshold E_{min}^{had} depends on where the one-dimensional assumption is not valid anymore for the hadronic part of the shower. In order to test this we show in Fig. 6 the longitudinal and lateral and distribution function of muons, which are direct decay products of pions and kaons. A value of $E_{min}^{had} = 10^4 GeV$ provides sufficient precision for both profiles.

B. Tests on a single shower basis

By evolving the high energy part of a shower with the MC-method, we are able to reproduce the natural fluctuations, which are primarily due to the varying depth of the first interactions. All particles which fall below a threshold fE_0 are used in the initial condition for the CE. In order to show that the CE are solved correctly for an arbitrary initial condition, we compare to the MC method by computing the high energy part in exactly

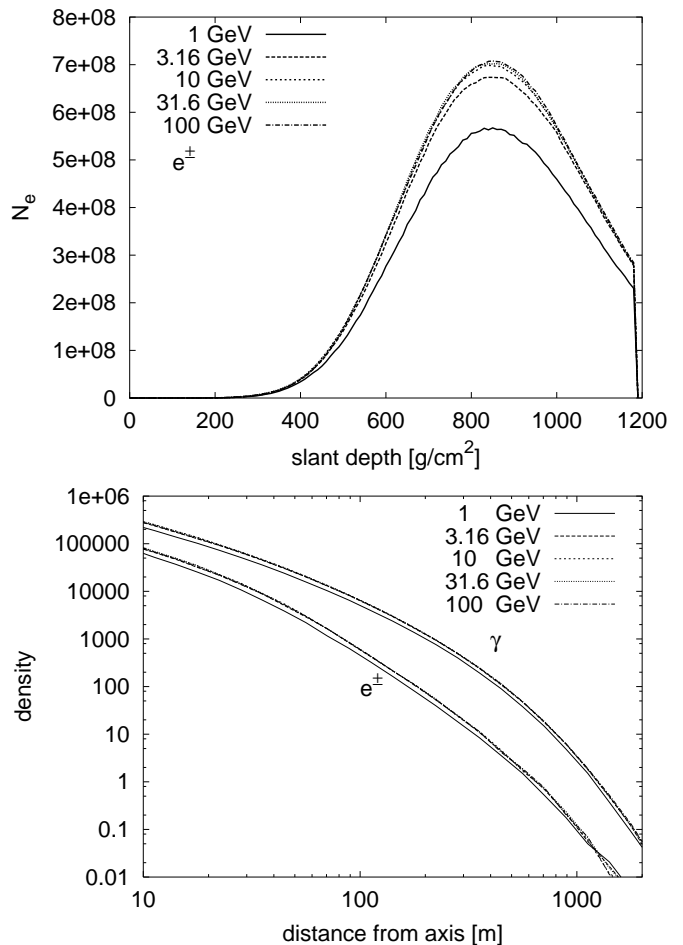


FIG. 5: Longitudinal profile of electrons and positrons (upper figure) and the lateral distribution function (lower figure) of electrons/positrons (lower curves) and photons (upper curves) for a photon induced shower and different values of E_{min}^{em} . In the lateral case, the four curves for $E_{min}^{em} > 3.16 GeV$ are indistinguishable.

the same way for both approaches. Technically this can be done by choosing the same seed for the pseudo random number generator in the computer program. Fig. 7 shows such a comparison for the longitudinal and lateral profile of electrons and positrons. The thinning level for the MC method is 10^{-7} . We see a slight sensitivity of the longitudinal profile to the number of bins used in the numerical solution of the cascade equations. The shower maxima are at 738, 742, 739, and 740 g/cm^2 for the MC method, and the 10, 30 and 50 bin solution of the CE, respectively. The lateral distribution function is very insensitive to the number of bins.

C. Statistical properties - fluctuations

Next, we compare the statistical properties of two sets of proton induced $10^{19} eV$ showers calculated with CE

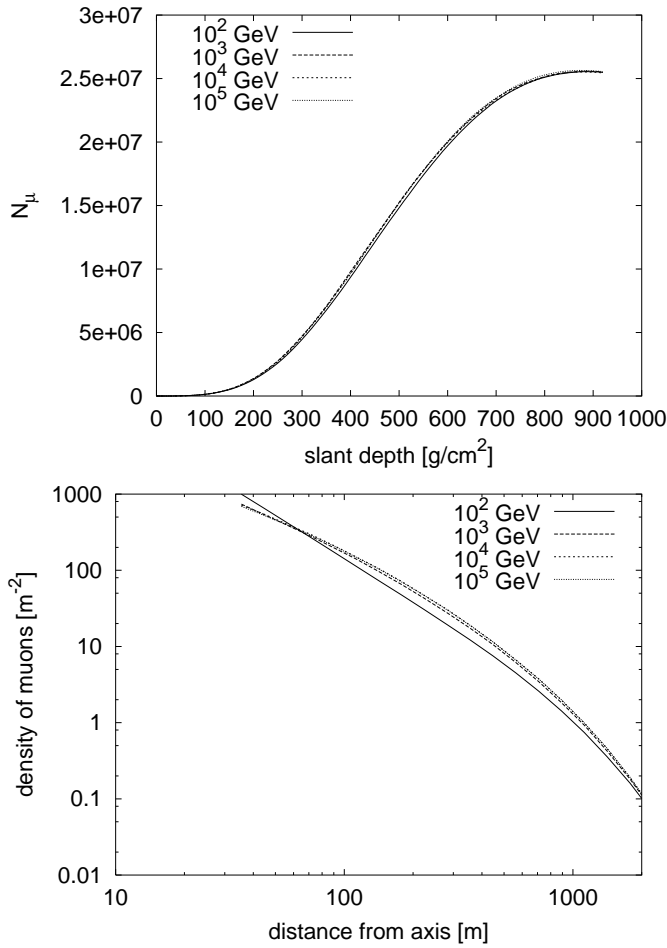


FIG. 6: The dependence of longitudinal and lateral profiles of muons as a function of E_{\min}^{had} . In the lateral case, the two curves for $E_{\min}^{\text{had}} \geq 10^4 \text{ GeV}$ are indistinguishable.

(500 showers) and MC-method (500 showers, 10^{-5} thinning). In Fig. 8 one sees the distribution of the shower maxima for the MC and CE methods. The two distributions agree well. The threshold f , where CE takes the initial condition from the high energy MC part and computes the shower numerically, was chosen to be 0.001. The influence of the parameter f on the fluctuations is shown in Fig. 9, by plotting $\sigma = \sqrt{\langle X_{\max}^2 \rangle - \langle X_{\max} \rangle^2}$ against f . The smaller the value of f , the further the initial portions of the shower is followed exactly rather than with the CE. We see that even for f approaching unity, the fluctuations seen at small f are reproduced to a great extent. This shows that natural fluctuations arise for the most part from the depth of the first interaction of the cosmic ray in the atmosphere.

D. Comparisons with CORSIKA

Finally, we compare some of our results to CORSIKA simulations. CORSIKA [13] is a well tested simula-

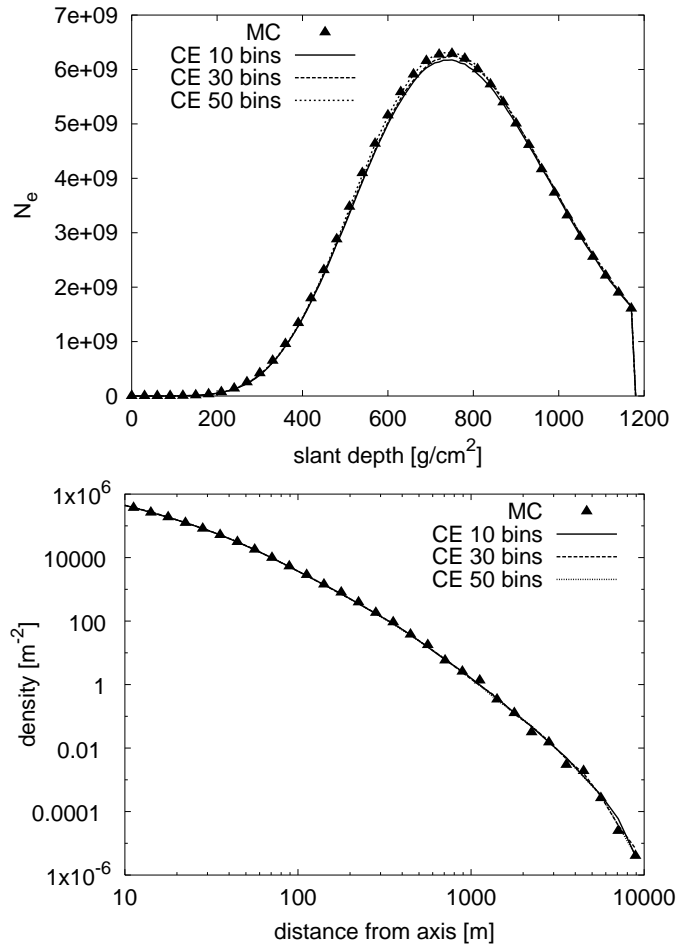


FIG. 7: An example of a shower calculated in the same way to down to $0.001E_0$, using below MC method (triangles) with 10^{-7} thinning, or CE with different binnings.

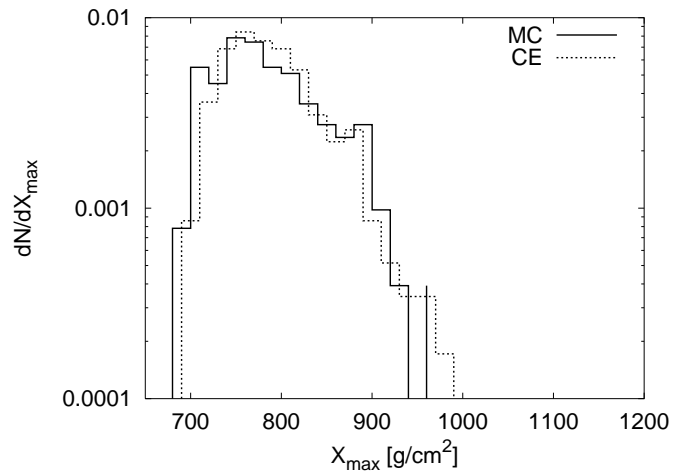


FIG. 8: Comparison of a shower maximum distribution for 10^{19} eV proton induced showers.

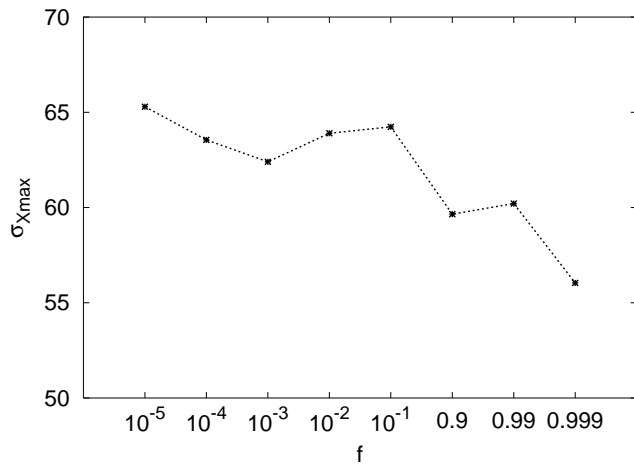


FIG. 9: The fluctuations of the shower maximum $\sigma = \sqrt{\langle X_{\max}^2 \rangle - \langle X_{\max} \rangle^2}$ as a function of the fractional energy threshold. 1000 showers have been calculated for each value of f .

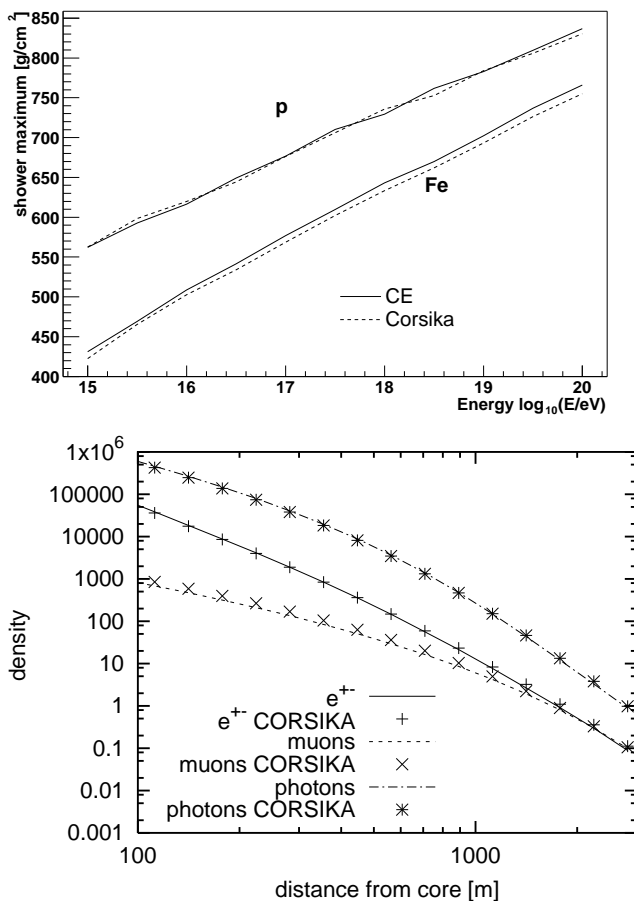


FIG. 10: Comparison to CORSIKA: the shower maximum as a function of the primary energy (top figure) for 30 degree inclined proton and Fe showers and the lateral distribution function for the average of ten 5×10^{19} eV proton induced vertical showers (bottom figure).

tion package, which can be configured to use the same external models employed here for our hybrid model: QGSJET for the high energy hadronic part, GHEISHA for low energy hadrons and EGS4 for the electromagnetic part. Fig. 10 shows in the upper panel a comparison of the shower maximum for proton and iron induced 30-degree inclined showers. The shower proton curves agree nicely; the iron curve is slightly higher in our case. This might be due to differences in the computation of nucleus-nucleus cross sections, which are calculated from nucleon-nucleon cross sections using the Glauber method. We use $f_{\max}^{\text{had}} = 0.001 < 1/56$ which avoids calculating the functions W_{mn} for all 56 possible nuclei. The lower panel compares the average lateral distributions functions of 5×10^{19} eV proton showers. They agree nicely for electrons/positrons and photons; compared to CORSIKA we produce slightly less muons, certainly due to the fact that we neglect photo-nuclear reactions at this stage.

E. Summary

We introduced a hybrid approach to air shower simulations which uses cascade equations as proposed in reference [8]. This method consists of applying traditional Monte Carlo methods where natural fluctuations or the lateral spread of particles are important. Particles are passed to the cascade equations via the initial condition. The low energy source function obtained from the cascade equations provides the probability distribution of low energy particles, whose further propagation is followed by Monte Carlo. The hybrid approach takes advantage of the fast solutions of the cascade equations and provides detailed knowledge about each low energy particle, such as position, energy and arrival time.

Consistency checks have been made by comparing the hybrid CE approach to traditional Monte Carlo. The two methods agree nicely within a small error. The longitudinal profiles obtained with the CE approach are somewhat sensitive to the binning which enters in the numerical solution of the CE, if less than ≈ 30 bins per decade are used. The lateral distribution functions are very stable against these technical parameters.

The hybrid technique introduced here is faster than a traditional MC by at least a factor of 20 at 10^{19} eV.

Acknowledgments

This work was supported by NASA grant NAG-9246 and NSF grants NSF-PHY-9996173, and NSF-PHY-0101738. The computations were made on NYU's Mafalda: a Linux cluster financed in part by the Major Research Instrumentation grant NSF-PHY-0116590.

The authors thank D.Heck for providing X_{\max} data from CORSIKA simulations.

HJD would like to thank N.N.Kalmykov for introducing him into the subject of air shower simulations and

the permission to use his cascade equations code.

-
- [1] A.M. Hillas. In *Proc. 19th Int. Cosmic Ray Conf, La Jolla, USA*, volume 1, page 155, 1985.
- [2] N. N. Kalmykov and M. V. Motova. Calculation of longitudinal characteristics of eas from a primary fe-56 nucleus with account for production of a fireball in the quark - gluon plasma model. (in russian). *Yad. Fiz.*, 43:630–636, 1986.
- [3] Thomas K. Gaisser. *Cosmic Rays and Particle Physics*. Cambridge University Press, 1990.
- [4] L.G.Dedenko. *Can. J. Phys.*, 46:178, 1968.
- [5] A. A. Lagutin, A. V. Plyasheshnikov, V. V. Melenteva, R. I. Raikin, and A. Misaki. Lateral distribution of electrons in air showers. *Nucl. Phys. Proc. Suppl.*, 75A:290–292, 1999.
- [6] T.K. Gaisser, P.Lipari, and T.Stanev. In *Proc. 25th Int. Cosmic Ray Conf, Durban, South Africa*, 1997.
- [7] Jaime Alvarez-Muniz, Ralph Engel, T. K. Gaisser, Jefferson A. Ortiz, and Todor Stanev. Hybrid simulations of extensive air showers. *Phys. Rev.*, D66:033011, 2002.
- [8] G. Bossard et al. Cosmic Ray Air Shower Characteristics in the Framework of the Parton-based Gribov-Regge Model NEXUS. *Phys. Rev.*, D63, 2001.
- [9] N.N. Kalmykov, S.S. Ostapchenko, and A.I. Pavlov. *Nucl. Phys. B*, 17, 1997.
- [10] H.Fesefeldt. The simulation of hadronic showers. *PITHA 85/02*, Aachen 1985.
- [11] W. R. Nelson, H. Hirayama, and D.W.O. Rogers. *the EGS4 Code System*. SLAC-265, Stanford Linear Accelerator Center, 1985.
- [12] R. Brun, F. Bruyant, M. Maire, A. C. McPherson, and P. Zancarini. Geant3. *CERN DD/EE/84-1*, 1987.
- [13] D. Heck, J. Knapp, J.N. Capdevielle, G. Schatz, and T. Thouw. *Report FZKA 6019*, 1998.
- [14] A. N. Cillis, H. Fanchiotti, C. A. Garcia Canal, and S. J. Sciutto. Influence of the lpm effect and dielectric suppression on particle air showers. *Phys. Rev.*, D59:113012, 1999.